Torsions of *N*-Methylpyrrole and its Cation

Alexander R. Davies, David J. Kemp, and Timothy G. Wright[a]

School of Chemistry, University of Nottingham, University Park, Nottingham NG7 2RD, UK

Abstract

Torsional levels in *N*-methylpyrrole are investigated in the ground (S_0) and first excited (S_1) neutral states using two-dimensional laser-induced fluorescence (2D-LIF), and in the ground state cation (D_0^+) using zero-electron-kinetic-energy (ZEKE) spectroscopy. The ZEKE spectra confirm the largely Rydberg nature of the S_1 state. The activity seen in both the 2D-LIF and ZEKE spectra are indicative of vibronic (including torsional) interactions and torsional potentials in the three electronic states are deduced, and are consistent with calculated geometries. The adiabatic ionization energy of *N*-methylpyrrole is derived as 64202 $\pm$ 5 cm^{-1}.

Keywords

N-methylpyrrole, REMPI, ZEKE, 2D-LIF, torsion, fluorescence, ionization.

[a] Timothy G. Wright,

Professor of Physical and Theoretical Chemistry,

School of Chemistry,

University of Nottingham,

University Park,

Nottingham NG7 2RD

Phone: +44 115 8467076

FAX: +44 115 9513562

Email: Tim.Wright@nottingham.ac.uk

I. Introduction

Pyrroles, including *N*-methylpyrroles, are key building blocks of many biomolecules, medicines[1,2] and molecular wires.[3] As such, an understanding their energy-level structure underpins their photophysics and photodynamics. *N*-methylpyrrole (NMP), has been the subject of a number of spectroscopic and photodissociation studies.

The absorption spectrum at ambient temperature has been reported by Milazzo,[4] McDiarmid and Xing,[5] and Cooper et al.[6] Spectra of supersonic jet-cooled molecules have been presented by McDiarmid and Xing,[5] Philis[7,8] and Biswas et al.[9] A theoretical study of the torsional levels in NMP was published by Kanamaru[10], although we shall question the conclusions of this work. In addition, the photodynamics of NMP have been the subject of a number of studies.[11,12,13,14 15]

The low-lying electronic states of NMP are interesting, with occupied orbitals that are mixtures of valence and Rydberg-character. Initially, treating the methyl group as a point mass, the point group symmetry is C_{2v} and the ground electronic state configuration may be written as $\ldots a_1^2 b_1^2 a_2^2$, where the a_1 symmetry orbital is σ bonding, and the two outermost occupied orbitals are π bonding. At the S_0 optimized geometry, the lowest lying electronic states are largely Rydberg-like, and are formed following vertical excitations from the two outermost orbitals into these. Here, we locate the pyrrolyl ring in the *yz*-plane, with the N-CH_3 bond lying along the *z*-axis, then the symmetry of the Rydberg states are 3s (a_1), 3p$_x$ (b_1), 3p$_y$ (b_2) and 3p$_z$ (a_1). We shall come back to these later, but here we note that the lowest-energy vertical excitation is the 3s $\leftarrow a_2$ excitation, yielding the S_1 $^1A_2$ first excited state; the highest occupied orbital in the S_1 state evolves from 3s character in the Franck-Condon region, to σ^* character at extended N-CH_3 bond lengths.[14] Accessing this state is electronically forbidden in a one-photon transition, although it has been seen in two-photon transitions in some of the above-cited work; as such, the activity seen in the one-photon spectrum is induced by vibronic interactions.

The main focus of the present work will be the torsional levels in the S_0, S_1 and D_0^+ electronic states. The torsional levels in the S_1 state have been assigned on the basis of activity seen in the resonance-enhanced multiphoton ionization (REMPI) spectrum of internally cold NMP by Philis;[7] further, the observation of hot-band structure also allowed information on the S_0 state to be obtained; we shall compare our results to those. For the first time, we shall also present zero-electron-kinetic energy (ZEKE) spectra using S_1 torsional levels as intermediates, allowing the torsional levels in the cation to be investigated.

II. Experimental

The REMPI/ZEKE[16] and 2D-LIF[17] apparatuses are the same as those employed recently. In both experiments, a free-jet expansion of NMP (Sigma-Aldrich, 99% purity) in 2 bar Ar was employed.

For the 2D-LIF spectra, the free-jet expansion was intersected at *X*/*D* ~20 by the frequency-doubled output of a single dye laser (Sirah CobraStretch), operating with Coumarin 480 and pumped with the third harmonic of a Surelite III Nd:YAG laser. The fluorescence was collected, collimated, and focused onto the entrance slits of a 1.5 m Czerny-Turner spectrometer (Sciencetech 9150) operating in single-pass mode, dispersed by a 3600 groove/mm grating, allowing ~300 cm^{-1} windows of the dispersed fluorescence to be collected by a CCD camera (Andor iStar DH334T). At a fixed grating angle of the spectrometer, the excitation laser was scanned, and at each excitation wavenumber the camera image was accumulated for 2000 laser shots. This allowed a plot to be produced of fluorescence intensity versus both the excitation laser wavenumber and the wavenumber of the emitted and dispersed fluorescence, termed a 2D-LIF spectrum. [18,19]

For the REMPI and ZEKE spectra of NMP, the focused outputs of two dye lasers (Sirah CobraStretch) were overlapped spatially and temporally, and passed through a vacuum chamber coaxially and counterpropagating, where they intersected the free jet expansion. The excitation laser operated with Coumarin 480 and was pumped with the third harmonic (355 nm) of a Surelite III Nd:YAG laser and was frequency doubled while the ionization laser operated with Coumarin 440, pumped with the third harmonic (355 nm) of a Surelite I Nd:YAG laser, and was undoubled. The jet expansion passed between two biased electrical grids located in the extraction region of a time-of-flight mass spectrometer, which was employed in the REMPI experiments. These grids were also used in the ZEKE experiments by application of pulsed voltages, giving typical fields of ~10 V cm^{-1}, after a delay of up to 2 μs; this delay was minimized while avoiding the introduction of excess noise from the prompt electron signal. The resulting ZEKE bands had widths of ~5-7 cm^{-1}. Electron and ion signals were recorded on separate sets of microchannel plates.

III. Results and Discussion

A. Overview

In Figure 1 we show the (1+1) REMPI spectrum of NMP over the first ~1000 cm^{-1}; the origin transition is located at 41193 cm^{-1} (Ref. 15). Here we concentrate on the 0–120 cm^{-1} wavenumber region, which is shown as an expanded trace. There are four cold bands in this region, which are assigned to transitions involving torsional levels. The (2+2) spectrum is also shown in Figure 1, and although this

is somewhat power broadened, as with other published versions of this,[9,15] it does allow the origin to be seen, as well as different vibrational structure to the (1+1) spectrum.

The torsional levels are described by the m quantum number, which is signed. Levels with $|m| \neq 3n$ ($n = 0, 1, 2\ldots$) are degenerate for a molecule that belongs to the G_{12} molecular symmetry group (MSG), while levels with $|m| = 3n$ are non-degenerate, forming linear combinations for $n \neq 0$; the $m = 0$ level is singly degenerate. The splitting of the $|m| = 3n$ ($n \neq 0$) levels occurs as a result of hindered rotation, caused by a torsional potential characterized by a parameter V_6. For example, the m = +3 and -3 levels, form combinations that are denoted 3(+) and 3(-), with their relative energy ordering determined by the sign of V_6, which arises from the minimum energy geometry. For geometries where the methyl group is eclipsed, with a C-H bond of the methyl group in the same plane as the pyrrolyl ring, V_6 is positive; while for a staggered geometry, where one of the methyl C-H bonds is perpendicular to the pyrrolyl ring, V_6 is negative.

As is well known, nuclear spin and symmetry considerations mean that it is not possible to cool the m = 1 torsional population into the m = 0 level, and hence under the jet-cooled conditions employed herein, both levels have roughly equal populations. As a consequence, transitions can occur from either the m = 0 or m = 1 level of the S_0 zero-point vibrational level. Since the separations of these two levels are very similar in the S_1 and S_0 electronic states, then the m^0 and m^1 bands are essentially coincident in the REMPI spectrum, and this will be true for all vibrational bands. (We will often refer to a level using the notation of a transition, e.g. a transition to S_1 m = 0 will be given by m^0; furthermore, we shall generally omit the initial level when designating a transition – with transitions to $m = 3n$ originating from the S_0 m= 0 level, and those for $m \neq 3n$ originating from S_0 $m = 1$ – subscripts refer to the S_0 state, superscripts to the S_1 state, and for cationic levels we use a pre-superscripted "+".)

In Figure 2, we show the low wavenumber region of the ZEKE spectra recorded via the four torsional levels in S_1 accessed via cold $S_1 \leftarrow S_0$ transitions. If the torsional potentials are very similar in the two electronic states, then we generally expect transitions that involve $\Delta m = 0$ to be the most intense, with $\Delta m = 3$ transitions possible, but expected to be much weaker; and the spectra clearly demonstrate this. From these ZEKE spectra, we can deduce the positions of the ${}^+m^0$, ${}^+m^1$, ${}^+m^2$, ${}^+m^{3(+)}$, ${}^+m^{3(-)}$ and ${}^+m^4$ levels. Note that, although the identification of the m^2 and m^4 bands in the REMPI spectrum are unambiguous, this is not the case for the $m^{3(+)}$ and $m^{3(-)}$ bands, which will be discussed below, although we can deduce that the ordering is the same in the S_1 and D_0^+ states.

In Figure 3, we present a 2D-LIF spectrum recorded over the region of the S_1 torsional levels, with the lowest excitation band only partially scanned. At the top of the 2D-LIF spectrum, we show the corresponding section of the REMPI spectrum from Figure 1, to indicate the excitation positions. Note that we have omitted the regions of the emission below ~60 cm^{-1}, where the $\Delta m = 0$ bands would be expected, as no features were discernible, suggesting that these are weak. We can see, however, emission bands to S_0 vibtor levels, and we see clear vibtor bands associated with several S_0 vibrational levels.

Again, the ordering of the S_1 $m^{3(+)}$ and $m^{3(-)}$ levels is not immediately clear, but we can deduce that the ordering is reversed between the S_0 and S_1 states, from the intensities of the emission bands in Figure 2.

B. Assignments and Discussion

We shall now switch the symmetry labels to those of the G_{12} MSG. (The correspondence between G_{12} and C_{2v} labels is given in Table 1.) We have noted in the above that electronic excitations and ionizations of a molecule that belongs to the G_{12} MSG generally obey a $\Delta m = 0$ selection rule. When referring to vibrations, we shall use a revised numbering based on the ring vibrations,[29] but the correspondence to the numbering employed in the work of Biswas et al.[9] is given in Table 2 for selected vibrations.

The REMPI spectrum for the $S_1 \leftarrow S_0$ transition corresponds to a $\tilde{A}^1A_2' \leftarrow \tilde{X}^1A_1'$ transition. The pure electronic transition is forbidden for a one-photon absorption, and hence the electronic origin does not appear in the (1+1) REMPI spectrum; furthermore, the torsional activity is expected to correspond to that which is facilitated by vibronic (Herzberg-Teller) coupling.

Philis[7] has given assignments of the four features in the expanded region of the (1+1) REMPI spectrum in Figure 1. We note that Kanamaru[10] has put forward a reinterpretation of the torsional transitions seen in Philis's work;[7] however, almost all of the proposed transitions are symmetry forbidden, and so we do not concur with this reassignment. We will conclude that the assignments given by Philis[7] are correct on the basis of the 2D-LIF and ZEKE spectra discussed herein.

In commenting on the torsional activity seen in the REMPI spectrum, we note that the missing electronic origin corresponds to the absence of both m^0 and m^1 transitions, which would be almost completely overlapped, since the effective rotational constant for CH_3 torsional motion is very similar in the two electronic states. As the one-photon $S_1 \leftarrow S_0$ transition is forbidden, the present bands must arise from a form of vibronic coupling which encompasses the torsional levels. (We generalize the use

of the term “vibronic” to cover vibration-electronic, torsion-electronic and vibration-torsion-electronic interactions.) There has been some slight confusion in discussing the vibrations and vibronic coupling in NMP, owing to different axis systems being employed, with the molecule having been located in the *yz*- and *xz*-planes (and perhaps both, on occasion!). In the present work, the pyrrolyl ring is located in the *yz*-plane throughout.

Wu et al.[14] have studied the low-lying states of NMP to explain observed photodynamics. The electronically-excited states of NMP are interesting, since they exhibit both Rydberg and valence character. Briefly, the ground electronic state of NMP is …$(a_2'')^2(a_2')^2$, with the HOMO and HOMO-1 orbitals corresponding to π orbitals. The lowest electronically-excited states are formed following excitation of electrons from these two orbitals into orbitals that are mostly Rydberg in character in the Franck-Condon region. The lowest Rydberg orbitals are 3s and $3p_{x,\,y,\,z}$ and the HOMO–HOMO-1 energy gap is quite similar to the 3s–3p energy gap. It was found[14] that the S_1 $^1A_2'$ state was the lowest in energy, and it is energetically well-separated from any higher states (by at least ~0.4 eV), while the states that arose from the $3p_{x,\,y,\,z} \leftarrow a_2'$ and $3s \leftarrow a_2''$ excitations all lay within a 0.5 eV window, when considering vertical excitations. The main character of these states and the oscillator strengths were also given for the transitions from the ground state. The S_2 state was calculated to arise mainly from the $3s \leftarrow a_2''$ excitation (yielding a $^1A_2''$ state), while the S_3–S_5 states arose mainly from the $3p_{x,\,y,\,z} \leftarrow a_2'$ excitations. Since the $3p_{x,\,y,\,z}$ orbitals have respective symmetries a_2'', a_1'' and a_1', then the resulting respective Rydberg states are $^1A_1''$, $^1A_2''$ and $^1A_2'$. (These correspond to the S_5, S_3 and S_4 states given in Ref. 14, respectively, but note that the symmetry for the S_5 state given therein is incorrect – this should be B_2 in C_{2v} symmetry, not A_1 as given therein.) The S_2 and S_3 states were calculated to be the closest in wavenumber to the S_1 state, and vibronic coupling would be expected to induce activity for transitions that involved torsional/vibrational levels of a_1'' symmetry. On the other hand, the S_5 state has an oscillator strength three times higher and is only 0.2 eV further removed in energy and this would be expected to induce activity for transitions that involved torsional/vibrational levels of a_2'' symmetry. Thus, interactions between S_1 and the $^1A_2''$ and $^1A_1''$ states can be used to rationalize the appearance of the $m^{3(+)}$ and $m^{3(-)}$ transitions, respectively – see below.

The symmetry arguments presented in the preceding paragraph refer to the m = 0 level of the interacting electronic state, however, similar arguments hold for the m = 1 level, which has e' symmetry for the S_2, S_3 and S_5 states. This means torsional (or vibtor) levels of the S_1 state of e' symmetry can have intensity induced through vibronic coupling, and this explains the appearance of the m^2 and m^4 transitions, as well as the absence of m^1 and m^5. We comment that the S_4 state cannot induce any activity, since transitions to it are also one-photon forbidden. Finally, the S_6 state of Ref.

14, arising largely from a $3p_x \leftarrow a_2''$ excitation, is an $^1A_1'$ state, and so could induce activity in transitions to the S_1 state involving torsion/vibrational levels of a_2' symmetry, which would include $m^{6(-)}$, but this would be expected to be weak, as the S_1 and S_6 states are almost 1 eV apart, and also the oscillator strength for the latter electronic state is fairly low. A very strong band at ~184 cm^{-1} in the REMPI spectrum (see Figure 1) was initially hypothesised to be the $m^{6(-)}$ transition,[7] but this assignment was revised in a later publication[9] – we shall comment on this further in due course.[29]

We now address the ordering of the m = 3(+) and m = 3(-) levels in the three electronic states. We have plotted the variation of the energies of the m levels with V_6 in Figure 4. (Note that the ordering of the m = 3n levels in Figure 4 is the reverse of that in Ref. 20.) We have already noted that the ordering is the same for the S_1 and D_0^+ states, but the reverse for the S_0 state. To establish the ordering, we have optimized the geometry of NMP in each of the three electronic states, and the optimized geometries are shown in Figure 5; Gaussian 16[21] was used for these calculations, with the level of theory and basis set shown. It is clear that the S_0 state is staggered, and both the S_1 and D_0^+ states are eclipsed. On this basis, the V_6 parameter is negative for the S_0 state and positive for the S_1 and D_0^+ states, as confirmed by the intensities in the 2D-LIF spectrum (Figure 3). This conclusion for the S_0 and S_1 states agree with the values deduced by Philis on the basis of hot and cold torsional transitions.[7] The ordering of the m= 3(+) and 3(-) levels in the three states is thus established and are labelled appropriately in Figures 1–3. The concurrence of the ordering in the S_1 and D_0^+ states is unsurprising, since the S_1 state is largely of 3s Rydberg character close to the Franck-Condon region, with its ionic core being the D_0^+ state; this is further confirmed by the largely diagonal nature of the torsional transitions during the ionization (see Figure 2). It is interesting to note that the $m^{3(+)}$ transition more intense than $m^{3(-)}$. This can gain intensity from $^1B_1 \leftarrow S_0$ transitions, and there are two such transitions close to the S_1 $^1A_2$ state.[14] Further, the $m^{3(-)}$ transition is more intense than it appears in similar spectra of substituted benzenes,[20,23] where its intensity arises from rotation-torsion coupling, (which is temperature dependent), since it cannot be vibronically induced. Here, this transition can gain intensity vibronically from a $^1B_2 \leftarrow S_0$ transition, which (once the correct symmetry is noted), corresponds to the strongest transition calculated in Ref. 14. This then explains why both the $m^{3(+)}$ and $m^{3(-)}$ transitions are observed. That the former is the more intense, presumably arises from the fact that there are two transitions from which to steal intensity, and these are energetically closest to the S_1 state; these two factors must outweigh the higher oscillator strength of the slightly higher-energy $^1B_2 \leftarrow S_0$ transition.

With regard to the magnitude of V_6, values of -45 cm^{-1} and 17 cm^{-1} have been deduced by Philis[7] for the S_0 and S_1 states, respectively; these gave a reasonable agreement with the observed line positions,

with the former value agreeing with a microwave study.[22] We have calculated the effective rotational constant, *F*, using the optimized geometries in Figure 5, and deduced the V_6 parameter from the positions of the *m* = 3(+) and *m*= 3(-) bands in the appropriate spectra. These values are given in Table 3, and for the S_0 and S_1 states agree well with those of Philis.[7] Caution is merited, however, since Lawrance and coworkers have shown that vibration-torsion interactions can affect the deduced V_6 (and *F*) values,[23,24] and so without further analysis, the present V_6 values must be viewed as being "effective" values. We note here that for the D_0^+ state, very similar potential parameters as the S_1 state provide satisfactory agreement with the observed ZEKE band positions, which is not unexpected as the S_1 state is Rydberg-like in the Franck-Condon region. For both the S_1 and D_0^+ states there is a low-lying a_2" symmetry vibration (16^1 at ca. 200 cm^{-1}) lying above the *m* = 3(+) and *m* = 3(-) levels,[29] with the latter level the higher. Comparing this situation to that of *p*FT (see Figure 6 of Ref. 23), we can expect vibration-torsion interactions to push the *m* = 3(-) level down towards the *m* = 3(+) level, with the latter remaining in approximately the same position; thus, the V_6 values in the S_1 and D_0^+ states are expected to be lower bounds to the true value. The opposite situation holds in the S_0 state, where the 3(-) level is the lower, so here the V_6 value is expected to be an upper bound.

The observation of the $^+m^0$ band in the ZEKE spectra (Figure 2) allows the adiabatic ionization energy (AIE) to be deduced. This value is 64202 $\pm$ 5 cm^{-1} (7.9600 $\pm$ 0.0006 eV), which compares well with previous experimental values of 7.94$\pm$0.02 eV[6] and 7.95$\pm$0.05 eV.[25] Although we have no explanation why, we comment that we do not observe Δm = +3 bands in the ZEKE spectrum, only Δm = -3 bands, even though both symmetry-forbidden bands can be induced by vibronic coupling in the cation/high-lying Rydberg states, or by intrachannel coupling.[26]

Going back to the 2D-LIF spectrum in Figure 3, we have noted that we do not see emission to the torsional levels in S_0, only to vibtor levels. These are assigned based on previous IR/Raman values[27,28] (see also Ref. 9) and further fluorescence spectra to be published.[29] They are consistent with a value of V_6 in S_0 in the range -40 cm^{-1} to -45 cm^{-1}, with the caveat that the vibtor levels are likely to be interacting. We particularly note the three bands to low emission wavenumber. The 236 and 259 cm^{-1} bands are in the correct position to be $16_1m_{3(-)}$ and $16_1m_{3(+)}$, respectively. The (46, 172) cm^{-1} band is difficult to assign, since it is not in the correct position for any calculated torsional level, and is lower than any vibrational wavenumber for the S_0 state. The only plausible explanation is that it arises from $m_{6(+)}$ or $m_{6(-)}$, which are perhaps interacting with one of the $16_1m_{3(-)}$ and $16_1m_{3(+)}$ levels, respectively; however, without a full analysis of the vibration-torsion interaction, this remains speculative.

IV. Conclusions

It has been established that the torsional levels in the NMP cation are almost identical to those in the S_1 state, and that the $\Delta m = 0$ propensity rule is closely followed, confirming that the latter is Rydberg-like in the Franck-Condon region. The observation of some $\Delta m = \pm 3$ transitions allows the accessing of the $^{+}m^{0}$ level in the ZEKE spectra, and this allows the AIE to be established as 64202 $\pm$ 5 cm^{-1}. The 2D-LIF spectrum confirms the S_1 state assignments and activity involving several ground state vibrations is observed. Furthermore, the observed (and unobserved) torsional activity has been rationalized both in terms of the calculated geometries, but also via the vibronic interactions.

In future work, a wide-ranging analysis of the S_0, S_1 and D_0^+ energy levels will be presented in a combined fluorescence and ZEKE study.[29]

Acknowledgements

We are grateful to the EPSRC for funding (grant EP/L021366/1). The EPSRC and the University of Nottingham are thanked for studentships to D.J.K. and A.R.D.

Data Availability Statement

The data that support the findings of this study are available from the corresponding author upon reasonable request.

Table 1: Correspondence of the C_{2v} point group symmetry classes with those of the G_{12} molecular symmetry group. Also indicated are the symmetries of the P_i vibrations and the different pure torsional levels.[a]

C_{2v}	G_{12}	P_i [b]	m
a_1	a_1'	$P_{1–9}$	0, 6(+)
a_2	a_2'	$P_{10–12}$	6(-)
b_1	a_2''	$P_{13–16}$	3(-)
b_2	a_1''	$P_{17–24}$	3(+)
	e'		2, 4
	e''		1, 5

[a] Symmetries of vibtor levels can be obtained by combining the vibrational symmetry (in G_{12}) with those of the pure torsional level, using the D_{3h} point group direct product table.

[b] The P_i vibrational labels will be described in a forthcoming publication.[29]

Table 2: Correspondence between the vibrational numbers used in the present work with those of Biswas et al.[9]

G_{12} (C_{2v}) Symmetry	Vibration numbering (present work)[29]	Vibrational numbering (Ref. 9)
a_1' (a_1)	6	8
a_2'' (b_1)	13	19
	14	20
	15	21
	16	22
a_1'' (b_2)	23	32

Table 3: Calculated *F* and experimental V_6 values (cm^{-1}) in the S_0, S_1 and D_0^+ states.[a]

m	S_0	S_1	D_0^+
F	5.39	5.27	5.35
V_6	-(40–45)[b]	14	10

[a] The *F* values used here have been calculated from the optimized geometries presented in Figure 5. The V_6 values are effective values (see text), and merely reproduce the spacing between the *m* = 3(+) and *m* = 3(-) states, with the appropriate sign. In the S_0 state, we have not observed the torsional levels themselves, but do see vibtor levels for different vibrations. The vibtor spacings could be affected by vibration-induced changes to the torsional potential and/or interactions between levels.

[b] Values vary slightly for vibtor levels associated with different vibrations – see Ref. 20 for a comment on vibration-modified torsional potentials.

Figure Captions

Figure 1

Black trace: (1+1) REMPI spectrum of NMP; grey trace (2+2) REMPI spectrum of NMP; full assignments will be presented in a forthcoming publication.[29] The origin transition is located at 41193 cm^{-1} (Ref. 15). An expansion of the low-wavenumber region of the (1+1) REMPI spectrum of NMP is also shown, which includes the torsional transitions. Assignments are discussed in the text.

Figure 2

ZEKE spectra via the S_1 torsional levels of NMP. Assignments are discussed in the text. The band positions relative to the $^+m^0$ or $^+m^1$ band positions are: $^+m^2$ (18 cm^{-1}); $^+m^{3(+)}$ (49 cm^{-1}); $^+m^{3(-)}$ (54 cm^{-1}); and $^+m^4$ (80 cm^{-1}). Derived F and V_6 positions are given in Table 3.

Figure 3

2D-LIF spectrum spanning the $S_1 \leftarrow S_0$ excitation region corresponding to the torsions. The origin transition is located at 41193 cm^{-1} (Ref. 15). Note that the m^2 level is only partially only partially shown, though it is expected from the band profiles in the REMPI trace (shown at the top of the figure) that the full band profile of the emissions from m^2 will closely resemble those from m^4. Assignments are discussed in the text. The lower-wavenumber emission region extending to the origin has not been included as no discernible features were seen.

Figure 4

Variation of the energies of the m levels for different values of V_6. Notice the switch in ordering of the $m = 3n$ (n = 1, 2) levels with the sign of V_6. V_6 is positive for the eclipsed confirmation (S_1 and D_0^+) states, and negative for the staggered conformation (S_0) – see Figure 5. For this plot, the torsional angle is taken as zero for the eclipsed conformation, and the effective torsional rotational constant was taken as 5.3 cm^{-1}. (Note that the ordering of the m = 3(+) and 3(-) levels is the reverse of that shown in Ref. 20.)

Figure 5

Optimized geometries of NMP and its cation, at the indicated levels of theory. Note that the methyl group of the S_0 state has an optimized staggered geometry, while the methyl group of the S_1 and D_0^+ states are both eclipsed, with respect to the pyrrolyl ring. These geometries were ascertained as minima by calculating the vibrational wavenumbers, which were all real – these will be discussed further in later work.[29]

Figure 1

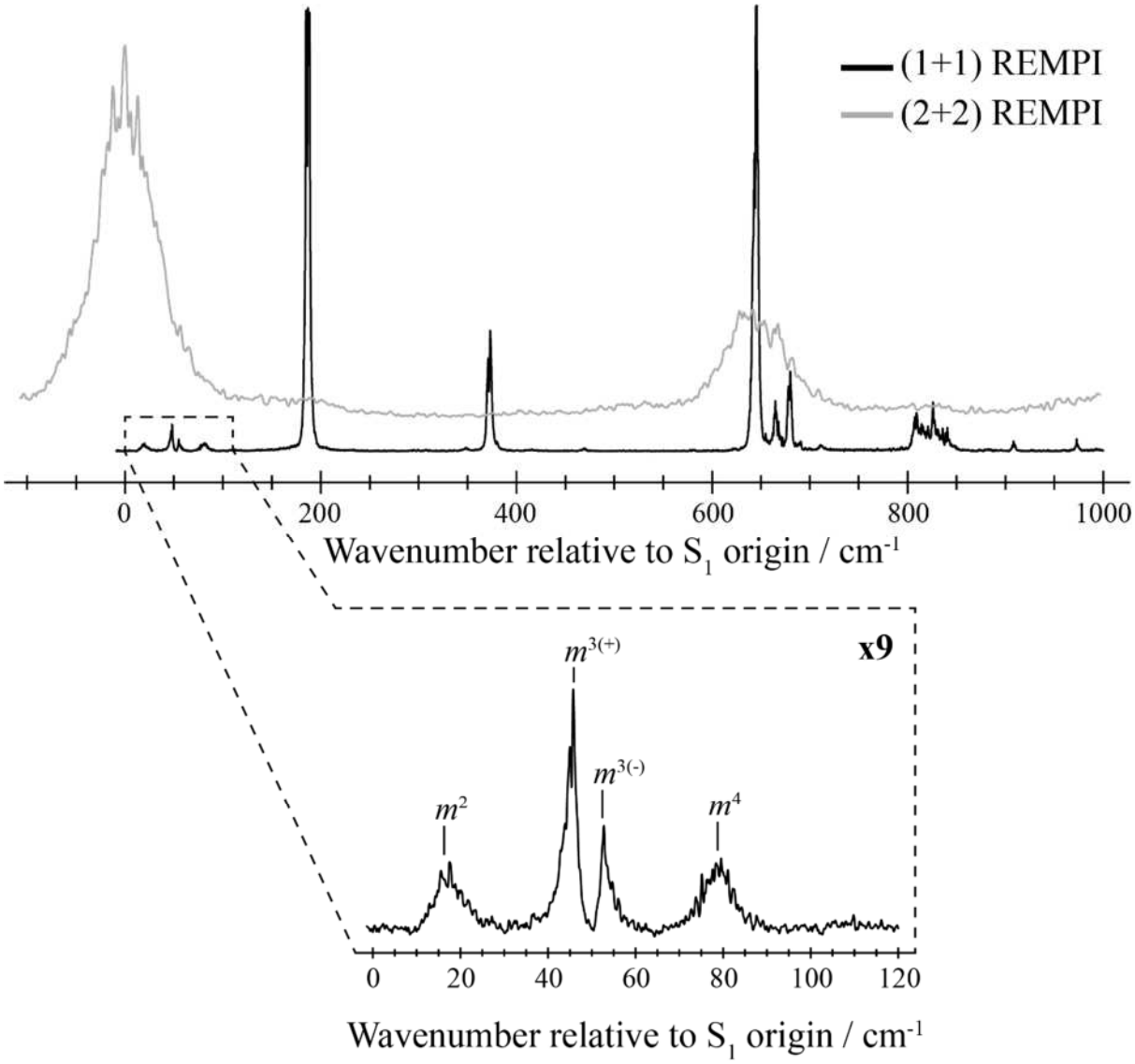
(1+1) REMPI
(2+2) REMPI
0
200
400
600
800
1000
Wavenumber relative to S1 origin / cm-1
x9
m3(+)
m3(-)
m2
m4
0
20
40
60
80
100
120
Wavenumber relative to S1 origin / cm-1

Figure 2

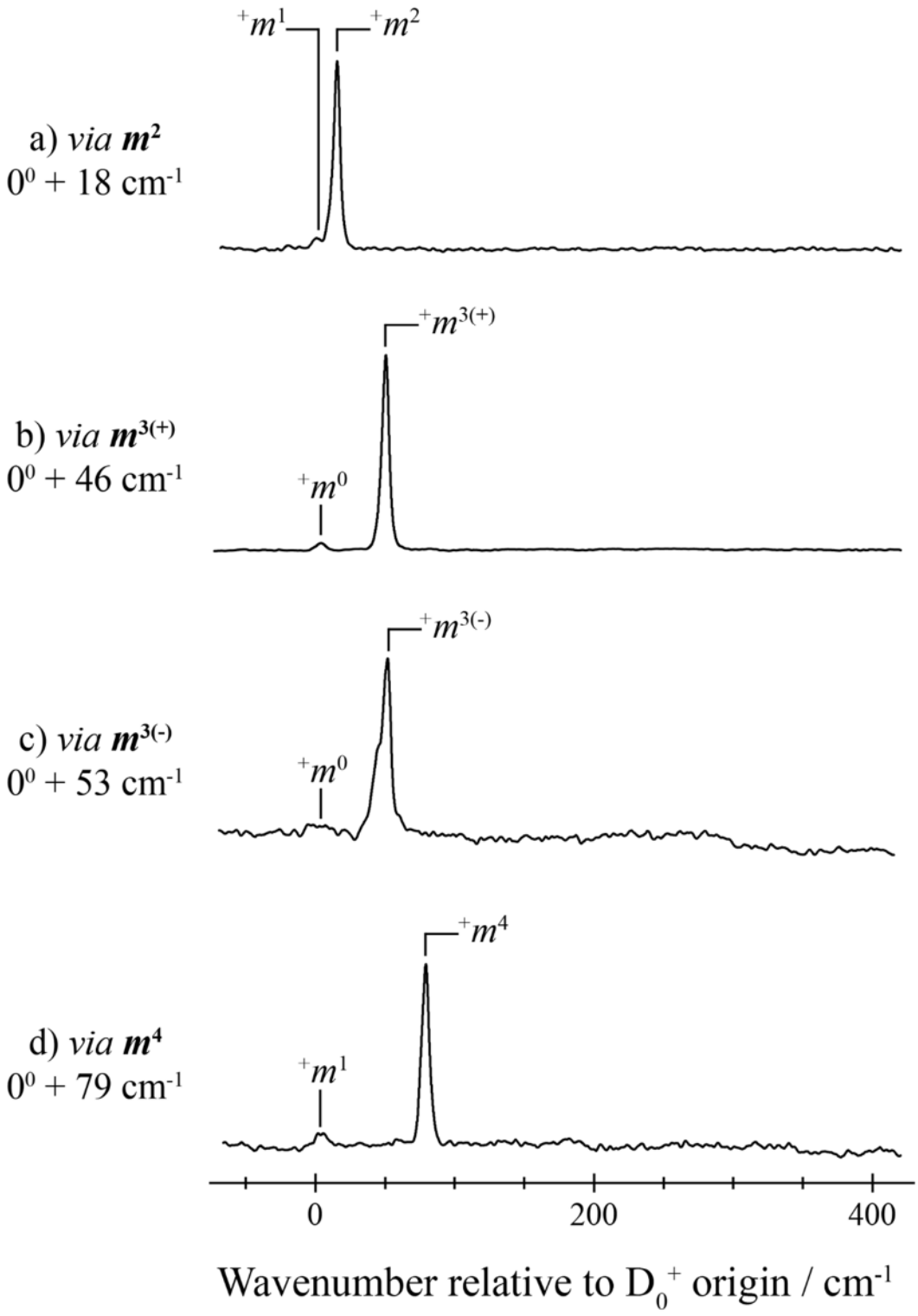
a) via m²
0⁰ + 18 cm⁻¹
+m¹
+m²
b) via m³(+)
0⁰ + 46 cm⁻¹
+m³(+)
+m⁰
c) via m³(-)
0⁰ + 53 cm⁻¹
+m³(-)
+m⁰
d) via m⁴
0⁰ + 79 cm⁻¹
+m⁴
+m¹
0
200
400
Wavenumber relative to D0+ origin / cm-1

Figure 3

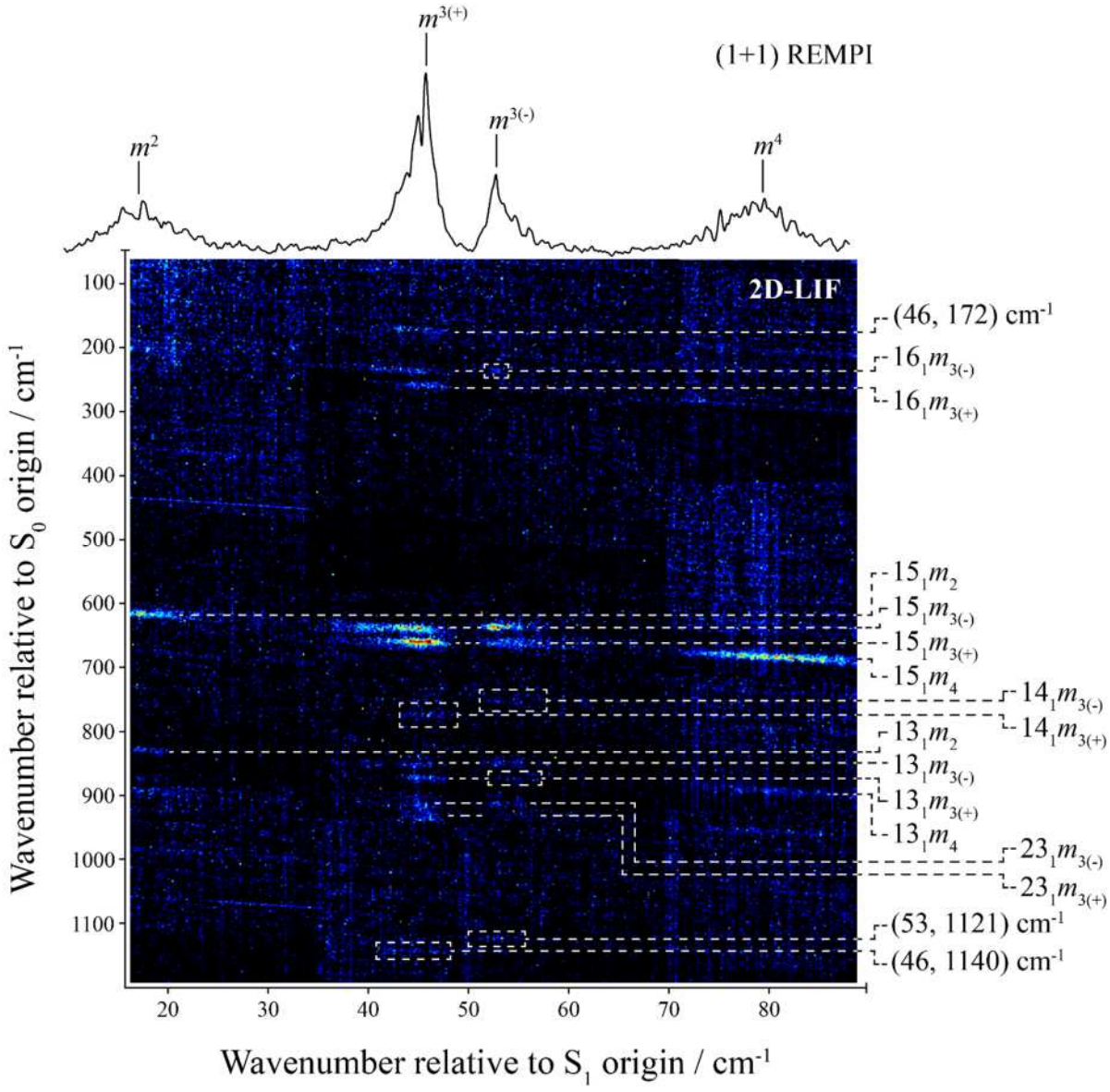
(1+1) REMPI
m^2
$m^{3(+)}$
$m^{3(-)}$
m^4
2D-LIF
(46, 172) cm^{-1}
$16_1m_{3(-)}$
$16_1m_{3(+)}$
15_1m_2
$15_1m_{3(-)}$
$15_1m_{3(+)}$
15_1m_4
$14_1m_{3(-)}$
$14_1m_{3(+)}$
13_1m_2
$13_1m_{3(-)}$
$13_1m_{3(+)}$
13_1m_4
$23_1m_{3(-)}$
$23_1m_{3(+)}$
(53, 1121) cm^{-1}
(46, 1140) cm^{-1}
Wavenumber relative to S_0 origin / cm^{-1}
Wavenumber relative to S_1 origin / cm^{-1}
100
200
300
400
500
600
700
800
900
1000
1100
20
30
40
50
60
70
80

Figure 4

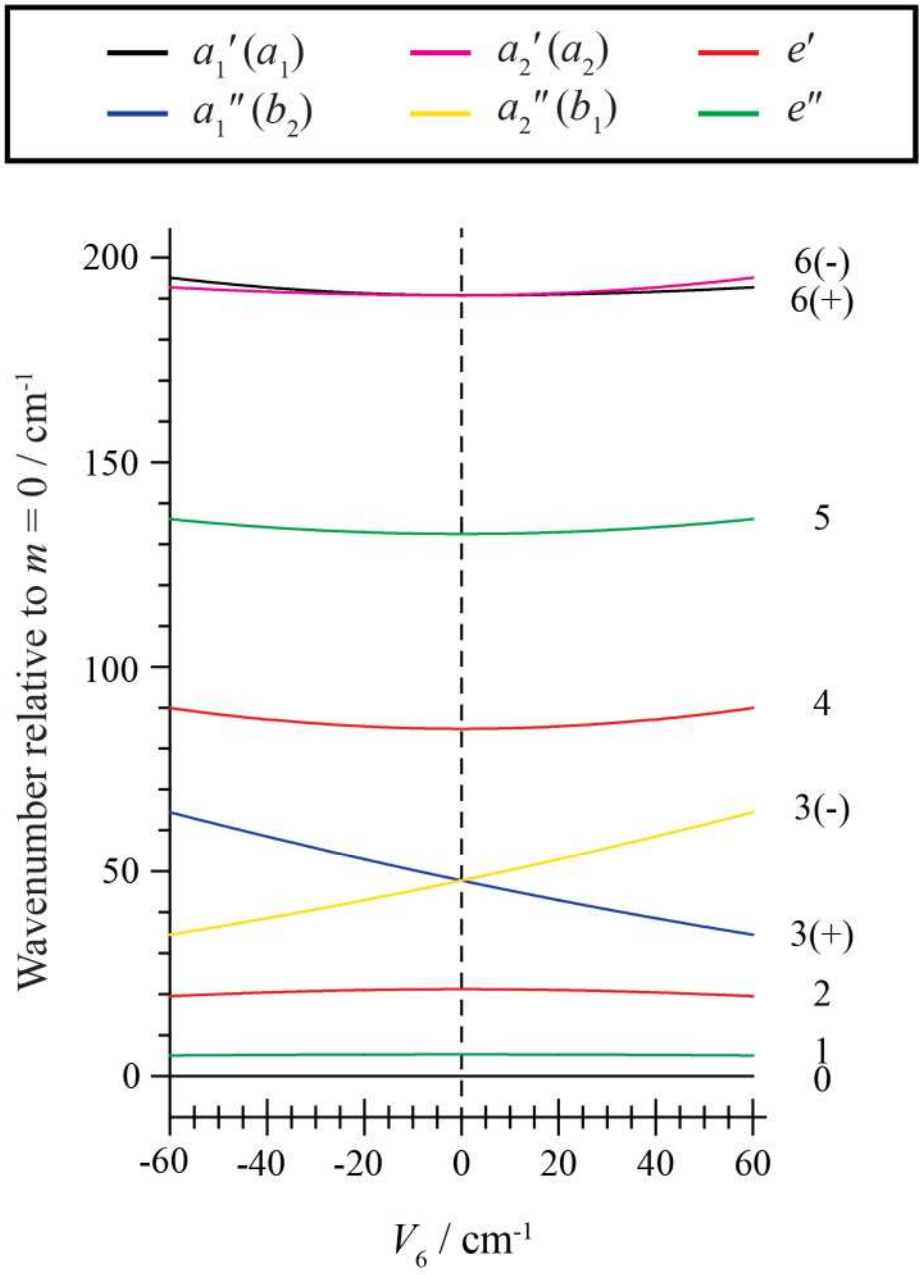
$a_1'(a_1)$
$a_2'(a_2)$
e'
$a_1''(b_2)$
$a_2''(b_1)$
e''
Wavenumber relative to m = 0 / cm^{-1}
200
150
100
50
0
-60
-40
-20
0
20
40
60
V_6 / cm^{-1}
6(-)
6(+)
5
4
3(-)
3(+)
2
1
0

Figure 5

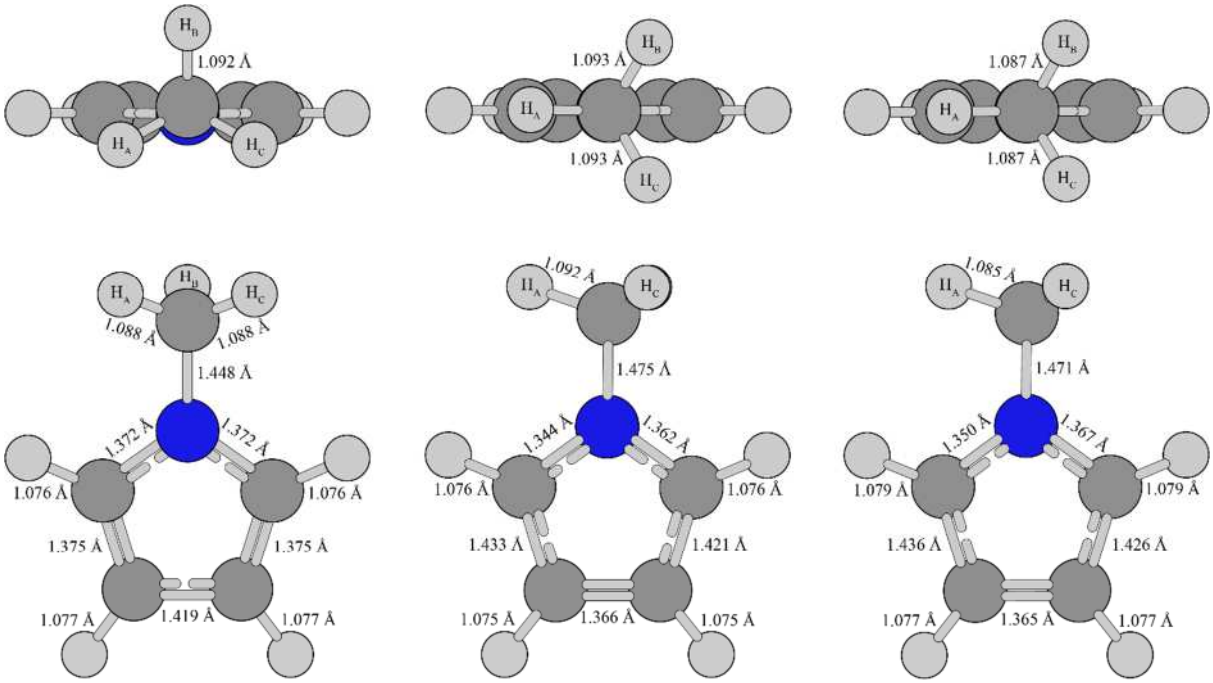

***N*-Methylpyrrole - S_0**
B3LYP / aug-cc-pVTZ
Geometry: staggered

***N*-Methylpyrrole - S_1**
TD-B3LYP / aug-cc-pVTZ
Geometry: eclipsed

***N*-Methylpyrrole - D_0^+**
U-B3LYP / aug-cc-pVTZ
Geometry: eclipsed

References

[1] V. Bhardwaj, D. Gumber, V. Abbot, S. Dhiman, and P. Sharma, RSC Adv. **5**, 15233 (2015).

[2] S. Chavda, K. Mulder, T. Brown, H. Makay, B. Babu, L. Westrate, A. Ferguson, S. Lin, K. Kiakos, J. P. Ramos, M. Munde, W. D. Wilson, J. A. Hartley and M. Lee, Med. Chem. **6**, 150 (2010)

[3] Y. Fu, X. Cheng, J. Zhao, T. Kong, C. Chi and X. Zhang, Polymer J. **44**, 1048 (2012).

[4] G. Milazzo, Gazz. Chim. Ital. **74**, 152 (1944).

[5] R. McDiarmid and X. Xing, J. Chem. Phys. **105**, 867 (1996).

[6] C. D. Cooper, A. D. Williamson, J. C. Miller, and R. N. Compton, J. Chem. Phys. **73**, 1527 (1980).

[7] J. G. Philis, Chem. Phys. Lett. **353**, 84 (2002).

[8] J. G. Philis, J. Molec. Struct. **651-653**, 567 (2003).

[9] N. Biswas, S. Wategaonkar, and J. G. Philis, Chem. Phys. **293**, 99 (2003).

[10] N. Kanamaru, J. Molec. Struct. (Theochem), **686**, 15 (2004).

[11] A. G. Sage, M. G. D. Nix, and M. N. R. Ashfold, Chem. Phys. **347**, 300 (2008).

[12] L. Blancafort, V. Ovejas, R. Montero, M. Fernández-Fernández, and A. Longarte, J. Phys. Chem. Lett. **7**, 1231 (2016).

[13] G. Piani, L. Rubio-Lago, M. A. Collier, T. Kitsopoulos, and M. Becucci, J. Phys. Chem. A **113**, 14554 (2009).

[14] G. Wu, S. P. Neville, O. Schalk, T. Sekikawa, M. N. R. Ashfold, G. A. Worth, and A. Stolow, J. Chem. Phys. **142**, 074302 (2015).

[15] K. C. Woo and S. K. Kim, Phys. Chem. Chem. Phys. **21**, 14387 (2019).

[16] V. L. Ayles, C. J. Hammond, D. E. Bergeron, O. J. Richards, and T. G. Wright, J. Chem. Phys. **126**, 244304 (2007).

[17] A. M. Gardner, W. D. Tuttle, L. E. Whalley, and T. G. Wright, Chem. Sci. **9**, 2270 (2018).

[18] N. J. Reilly, T. W. Schmidt, and S. H. Kable, J. Phys. Chem. A **110**, 12355 (2006).

[19] J. R. Gascooke and W. D. Lawrance, Eur. Phys. J. D **71**, 287 (2017).

[20] D. J. Kemp, E. F. Fryer, A. R. Davies and T. G. Wright, J. Chem. Phys. **151**, 084311 (2019).

[21] Gaussian 16, Revision A.03, M. J. Frisch, G. W. Trucks, H. B. Schlegel, G. E. Scuseria, M. A. Robb, J. R. Cheeseman, G. Scalmani, V. Barone, G. A. Petersson, H. Nakatsuji, X. Li, M. Caricato, A. V. Marenich, J. Bloino, B. G. Janesko, R. Gomperts, B. Mennucci, H. P. Hratchian, J. V. Ortiz, A. F. Izmaylov, J. L. Sonnenberg, D. Williams-Young, F. Ding, F. Lipparini, F. Egidi, J. Goings, B. Peng, A. Petrone, T. Henderson, D. Ranasinghe, V. G. Zakrzewski, J. Gao, N. Rega, G. Zheng, W. Liang, M. Hada, M. Ehara, K. Toyota, R. Fukuda, J. Hasegawa, M. Ishida, T. Nakajima, Y. Honda, O. Kitao, H. Nakai, T. Vreven, K. Throssell, J. A. Montgomery, Jr., J. E. Peralta, F. Ogliaro, M. J. Bearpark, J. J. Heyd, E. N. Brothers, K. N. Kudin, V. N. Staroverov, T. A. Keith, R. Kobayashi, J. Normand, K. Raghavachari,

A. P. Rendell, J. C. Burant, S. S. Iyengar, J. Tomasi, M. Cossi, J. M. Millam, M. Klene, C. Adamo, R. Cammi, J. W. Ochterski, R. L. Martin, K. Morokuma, O. Farkas, J. B. Foresman, and D. J. Fox, Gaussian, Inc., Wallingford CT, 2016.

[22] W. Arnold, H. Dreizler, and H. D. Rudolph, Z. Naturforsh. **23a**, 301 (1968).

[23] J. R. Gascooke, E. A. Virgo, and W. D. Lawrance, J. Chem. Phys. **143**, 044313 (2015).

[24] J. R. Gascooke and W. D. Lawrance, J. Molec. Spectrosc. **318**, 53 (2015)

[25] A. D. Baker, D. Betteridge, N. R. Kemp, and R. E. Kirby, Anal. Chem. **42**, 1064 (1970).

[26] D. J. Kemp, A. M. Gardner, W. D. Tuttle, J. Midgley, K. L. Reid and T. G. Wright, J. Chem. Phys. **149**, 094301 (2018).

[27] D. W. Scott, J. Mol. Spectrosc. **37**, 77 (1971).

[28] T. J. Dines, L. D. MacGregor, and C. H. Rochester, J. Coll. Int. Sci. **245**, 221 (2002).

[29] A. R. Davies, D. J. Kemp, and T. G. Wright (to be published).